Institute of Parasitology, Biology Centre CAS
Folia Parasitologica 2025, 72: 019
doi: 10.14411/fp.2025.019

Folia Parasitologica
http://folia.paru.cas.cz

Short Note OPEN ACCESS

Marginal cytokine modulation by *Schistosoma mansoni* soluble egg antigen in SARS-CoV-2-infected K18-hACE2 mice

Yi Mu[1,9], **Kexin Yan**[2,9], **Donald P. McManus**[1,10], **Wilson Nguyen**[2], **Daniel J. Rawle**[2], **Jason A. Roberts**[3,4,5,6], **Malcolm K. Jones**[1,7], **Pengfei Cai**[1,8]

[1] Molecular Parasitology Laboratory, QIMR Berghofer Medical Research Institute, Brisbane, Australia;

[2] Inflammation Biology, QIMR Berghofer Medical Research Institute, Brisbane, Australia;

[3] University of Queensland Centre for Clinical Research, Faculty of Medicine, University of Queensland, Brisbane, Australia;

[4] Herston Infectious Diseases Institute (HeIDI), Metro North Health, Brisbane, Australia;

[5] Departments of Pharmacy and Intensive Care Medicine, Royal Brisbane and Women's Hospital, Brisbane, Australia;

[6] Division of Anaesthesiology Critical Care Emergency and Pain Medicine, Nîmes University Hospital, University of Montpellier, Nîmes France

[7] School of Veterinary Science, University of Queensland, Brisbane, Australia;

[8] School of Biomedical Sciences, University of Queensland, Brisbane, Australia;

[9] These authors contributed equally to this work.

[10] Deceased

Abstract: Herein, we explore the potential influence of *Schistosoma mansoni* Sambon, 1907 soluble egg antigen (SmSEA) on the immunopathology of COVID-19 in K18-hACE2 mice infected with an Omicron BA.5 isolate of SARS-CoV-2. SmSEA treatment was delivered in a single dose by intraperitoneal injection, shortly after intrapulmonary inoculation of SARS-CoV-2. RNA-seq identified 36 differentially expressed genes in the spleens of virus-infected mice treated with SmSEA vs. PBS on day 5 post infection. Ingenuity Pathway Analysis of these genes suggested marginal modulation of cytokine responses, with upregulation of the IL-10 and IL-4 signatures and downregulation of the IFNγ signature. However, cytokine responses and histopathology in the lungs were largely unaffected. Future work will require purification of active helminth compounds and dosing and scheduling optimisation.

Keywords: COVID-19; severe acute respiratory syndrome coronavirus 2; schistosome; helminth-derived antigens; therapeutic immunomodulators; helminth therapy

This article contains supporting files (Figures S1,S2; Tables S1–S3) online at http://folia.paru.cas.cz/suppl/2025-72-019.pdf

Severe acute respiratory syndrome coronavirus 2 (SARS-CoV-2) emerged in late 2019 and is the etiological agent of coronavirus disease 2019 (COVID-19), a disease that affects more than 700 million people with over 7 million deaths. Severe COVID-19 is often associated with acute respiratory distress syndrome, which is characterised by the overproduction of pro-inflammatory cytokines, including tumor necrosis factor (TNF), interleukin-1 (IL-1), IL-2, IL-6, and interferon-gamma (IFNγ) (Qudus et al. 2023), a phenomenon often referred to as "cytokine storm" (Dharra et al. 2023). Myeloid cells are considered the main effector cells responsible for the hyperinflammatory responses associated with severe COVID-19 (Duan et al. 2024).

Parasitic helminths, especially soil-transmitted helminths, schistosomes and filarial worms, are among the most common human infections in developing countries (Hotez et al. 2008). Helminth infections typically promote T helper-2 (Th2) immunity and regulatory responses, characterised by the production of cytokines such as IL-4 and IL-5, and promotion of eosinophil responses, regulatory T cells (Tregs), IL-10-producing B cells (Bregs) and M2 macrophages (Girgis et al. 2013).

Some reports have suggested that helminth exposure may protect SARS-CoV-2 infection by counterbalancing excessive T helper-1 (Th1) responses (Wolday et al. 2021) or through macrophage-dependent T cell activation (Oyesola

Address for correspondence: Pengfei Cai, Molecular Parasitology Laboratory, QIMR Berghofer Medical Research Institute, 300 Herston Rd, Herston, Queensland 4006, Australia. E-mail: Pengfei.Cai@qimrberghofer.edu.au. ORCID: 0000-0003-4975-4615

et al. 2023). However, compelling evidence for effective immunotherapy of COVID-19 via helminth-derived products (HDPs) is limited, although several HDPs have been proposed as potential therapeutic immunomodulators (Siles-Lucas et al. 2021, Adjobimey et al. 2022, Cai et al. 2022, Serrat et al. 2023, Cao et al. 2024). *Schistosoma mansoni* soluble egg antigen (SmSEA) can drive strong Th2 polarising activity and induce the development of IL-10-producing Breg and Treg cells *in vivo* (Haeberlein et al. 2017).

In this study, we sought to determine whether SmSEA might be used as an immunotherapeutic for COVID-19-related lung inflammation, using the K18-hACE2 mouse model of infection and disease. The latter recapitulates the pro-inflammatory pathways observed in human COVID-19 (Bishop et al. 2022).

To generate *S. mansoni* eggs, Swiss mice were anaesthetised prior to percutaneous exposure to infectious schistosome cercariae (~150–170 per mouse) freshly shed from freshwater *Biomphalaria glabrata* (Say) snails (Fogarty et al. 2019). All animal protocols were approved by the QIMR Berghofer Medical Research Institute (QIMRB) Animal Ethics Committee (project number: P3818) and the experiments were carried out in accordance with NHMRC guidelines.

Live parasites were placed in contact with the skin of the mouse and allowed to penetrate naturally. At 7 weeks post infection, the mice were euthanised and the liver tissues were removed for egg isolation. The liver tissues were chopped with a scalpel blade to a smooth consistency.

The pellet was resuspended in 50 ml PBS containing 20 mg collagenase B, 125 mg trypsin, 10 µg penicillin and 20 µg streptomycin, and then incubated at 37 °C overnight with gentle shaking. After centrifugation at 400 × *g* for 5 min, the supernatant was removed, and the pellet was resuspended in 50 ml fresh PBS. After repeated washes with PBS, the pellet was resuspended in 25 ml fresh PBS. The suspension was successively passed through 250- and 150-µm mesh metal sieves.

The filtrate was centrifuged at 400 × *g* for 5 min and the supernatant was removed. The egg pellet was resuspended in 10 ml PBS and layered onto the top of a Percoll column (containing a mixture of 8 ml of Percoll and 32 ml of 0.25 M sucrose in a 50 ml tube). After centrifugation at 800 × *g* for 10 min at 4 °C, the liver cells/debris in the supernatant was removed. The eggs were resuspended in 25 ml PBS containing 1 mM EDTA and 1 mM EGTA. After centrifugation at 400 × *g* for 3 min, the supernatant was discarded and the pellet was mixed with 10 ml of the above buffer, and spun at 400 × *g* for 3 min.

After repeating the above step, the egg pellet was resuspended in 5 ml PBS and applied on to the second Percoll column (containing a mixture of 2.5 ml of Percoll and 7.5 ml of 0.25 M sucrose in a 15 ml tube). After centrifugation at 800 × *g* for 10 min at 4 °C, the supernatant was removed and egg pellet was resuspended in 10 ml PBS and spun at 400 × *g* for 3 min, and the wash was repeated three times. The egg pellet was washed three times with PBS and then transferred to 1.5 ml tubes. The purity and integrity of the isolated eggs were confirmed under a light microscope (Supplementary Fig. S1A).

SmSEA was prepared from the isolated eggs as previously described (Mohammed et al. 2020). Briefly, the purified eggs were resuspended in 5 ml of cold LPS-free PBS (Thermo Fisher Scientific, Scoresby, Australia) at a concentration of 100,000 eggs/ml. The suspended eggs were sonicated for 15 min on ice until more than 95% were destroyed. The homogenised eggs were centrifuged at 2,000 × *g* for 20 min at 4 °C. The supernatant was collected in a sterile tube and then centrifuged at 20,000 × *g* for 1 hr at 4 °C. The supernatant was filtered through a syringe filter unit (0.22 µm) and the concentration of SmSEA was determined using the Qubit Protein Assay Kit (Thermo Fisher Scientific, Scoresby, Australia).

The endotoxin concentration in SmSEA was measured with a Pierce™ Chromogenic Endotoxin Quant Kit (Thermo Fisher Scientific, Scoresby, Australia). The sample was electrophoresed on a 12% Mini-PROTEAN TGX precast gel (Bio-Rad Laboratories, South Granville, Australia) to observe the protein band pattern of SmSEA (Supplementary Fig. S1B). A portion of SmSEA was heat inactivated at 80 °C for 20 min, then immediately chilled on ice and stored at –80 °C until use.

Viral titres for omicron BA.5 were determined using CCID50 assays as described by Rawle et al. (2021). Briefly, Vero E6 cells were diluted to 2×10^2 cells/µl medium (RPMI 1640 supplemented with 2% FCS), and placed in 96 well plates (100 µl per well). The SARS-CoV-2 virus-infected cell culture supernatant was diluted in 10-fold serial in 100 µl of medium and the diluent serial were added to Vero E6 cells, which were cultured at 37 ˚C in the incubator supplied with 5% of CO_2 for 5 days. The virus titre was determined by the Spearman-Karber method.

To evaluate the potential immunomodulatory effects of SmSEA, three groups of female K18-homozygous hACE2 mice received intrapulmonary infections via the intranasal route (while under light anaesthesia) with an Omicron BA.5 isolate of SARS-CoV-2 (5×10^4 $CCID_{50}$ in 50 µl RPMI 1640 medium per mouse) as described previously (Stewart et al. 2023). There were six mice per group, aged 9–28 weeks, with a similar mean age and age distribution in each group. The mice were allowed to recover from anaesthesia, and then received PBS (50 µl), SmSEA (50 µg in 50 µl), or heat-inactivated SmSEA (hiSmSEA, 50 µg in 50 µl) via intraperitoneal injection (approximately 1 hr post infection).

Mouse body weight was measured before virus infection and at 3, 4, and 5 days post infection (dpi), with no significant differences in weight loss observed between the groups (Fig. 1A). The mice were euthanised at 5 dpi, and the virus titres in the lung, nasal turbinate and brain tissues were determined as previously described (Stewart et al. 2023). The only significant difference in tissue viral titres was in nasal turbinates for the hiSmSEA and PBS treatments (Fig. 1B).

To evaluate overt effects on lung consolidation, parenchymal white space analysis was performed using scanned (Aperio AT Turbo, Aperio, Vista, California, USA) H & E-stained lung sections (Fig. 1C) and QuPath v0.2.3 software as described previously (Dumenil et al. 2023). Although SmSEA treatment had no significant effect, hiSmSEA treatment significantly reduced the fraction of white space in the lung pa-

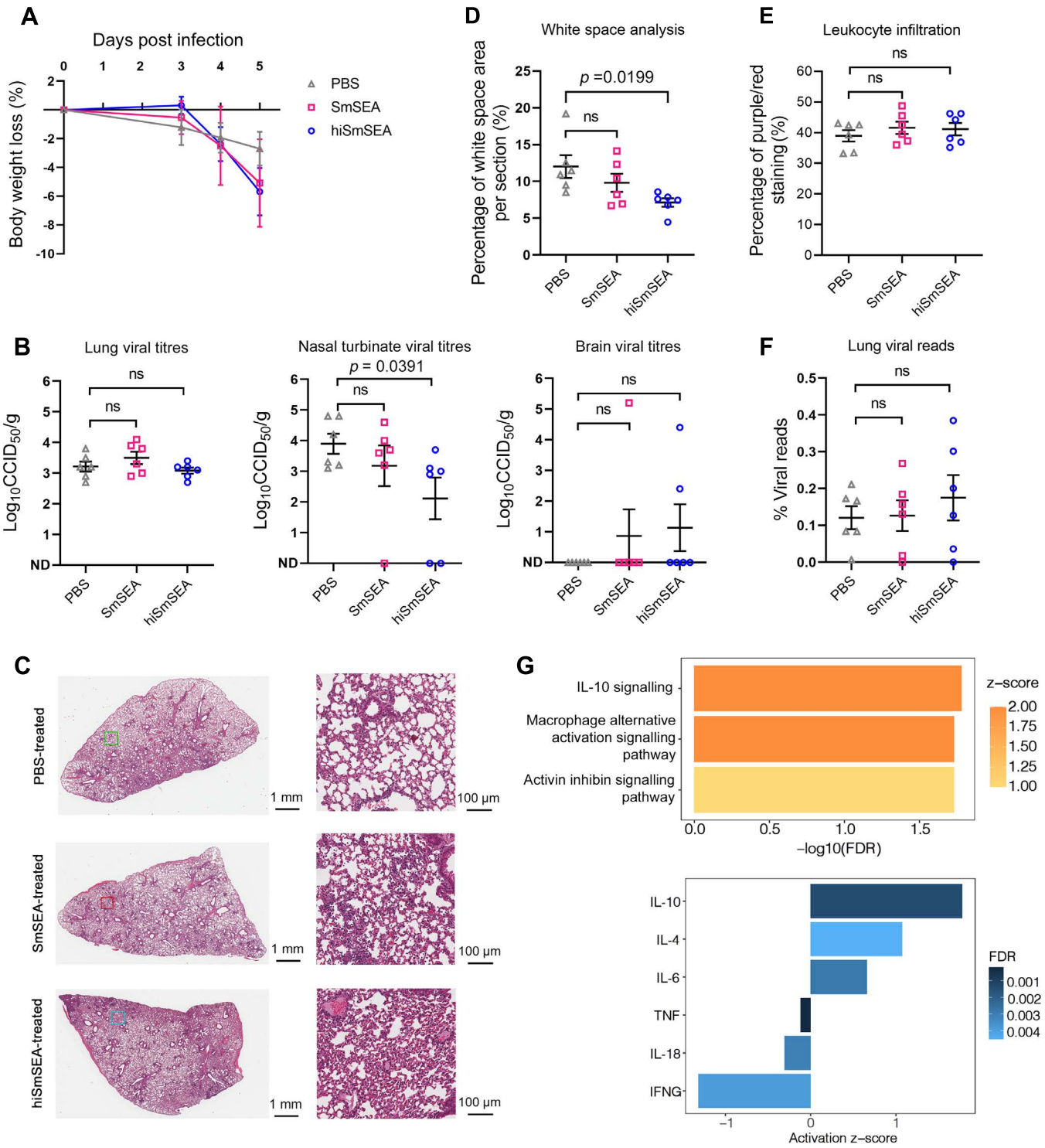

Fig. 1. A – percentage of body weight change in mice infected with SARS-CoV-2 followed by SmSEA, hiSmSEA or PBS treatment; **B** – tissue virus titres in the indicated tissues determined by $CCID_{50}$ assay at 5 dpi (ND, not detected); **C** – representative images of H & E-stained lung sections from mice infected with SARS-CoV-2 BA.5 and treated with PBS (upper panels), SmSEA (middle panels) and hiSmSEA (lower panels) at 5 dpi. Examples of areas of white space are indicated by coloured squares; **D** – white space analysis of H & E-stained lung sections, a measure of lung consolidation; **E** – aperio pixel count of purple (nuclear) over red (cytoplasmic) staining, a measure of leukocyte infiltration; **F** – the percentage of viral reads out of total clean reads in lung tissue at 5 dpi determined using RNA-seq; **G** – RNA-seq analysis of spleen samples from SARS-CoV-2-infected mice treated with SmSEA vs. PBS identified 36 Differentially Expressed Genes (DEGs), which were analysed by Ingenuity Pathway Analysis (IPA). The upper panel shows significantly enriched canonical pathways (FDR < 0.05), and the lower panel shows key inflammatory cytokines predicted as upstream regulators based on IPA Core Analysis. (Panels A, D and E, One-Way ANOVA followed by Turkey's comparison; Panels B and F, Kruskal–Wallis test followed by Dunn's comparison; n = 6 per group for all analyses; ns, no significance).

Table 1. Splenic Differentially Expressed Genes (DEGs) identified between SARS-CoV-2-infected mice treated with SmSEA and those treated with PBS (control) using edgeR.

Ensembl gene ID	Gene name	logFC	logCPM	P Value	FDR
DEGs upregulated in SmSEA-treated group (FDR < 0.05, logFC > 0)					
ENSMUSG00000020108	*Ddit4*	1.4100027	6.648323	5.3610E-09	8.0228E-05
ENSMUSG00000045382	*Cxcr4*	1.0737127	6.98207	3.3228E-08	2.4863E-04
ENSMUSG00000024042	*Sik1*	0.9586609	6.441928	5.0273E-08	2.5078E-04
ENSMUSG00000050075	*Gpr171*	0.5275645	5.425038	6.7266E-08	2.5166E-04
ENSMUSG00000024190	*Dusp1*	0.9372062	5.333836	1.1506E-07	3.4436E-04
ENSMUSG00000031431	*Tsc22d3*	1.0535411	7.748562	9.6804E-07	2.4145E-03
ENSMUSG00000026121	*Sema4c*	0.4257101	4.829532	3.5380E-06	6.0348E-03
ENSMUSG00000014773	*Dll1*	0.359489	6.007806	3.6293E-06	6.0348E-03
ENSMUSG00000029135	*Fosl2*	0.5872802	4.979752	6.7216E-06	1.0059E-02
ENSMUSG00000045817	*Zfp36l2*	0.6268494	7.721205	1.1490E-05	1.5632E-02
ENSMUSG00000032089	*Il10ra*	0.2951876	7.796179	2.1516E-05	1.9369E-02
ENSMUSG00000079560	*Hoxa3*	0.7682241	1.220575	2.2002E-05	1.9369E-02
ENSMUSG00000028967	*Errfi1*	1.0123704	5.123544	3.3233E-05	2.5725E-02
ENSMUSG00000006403	*Adamts4*	0.7330865	1.298229	3.4380E-05	2.5725E-02
ENSMUSG00000114278	*Gm49027*	1.1820509	-0.7295	3.8811E-05	2.6639E-02
ENSMUSG00000020181	*Nav3*	0.419236	2.573673	4.0173E-05	2.6639E-02
ENSMUSG00000054545	*Ugt1a6a*	0.8367139	2.170945	4.0942E-05	2.6639E-02
ENSMUSG00000039765	*Cc2d2a*	0.327445	2.997707	5.6589E-05	3.3775E-02
ENSMUSG00000038872	*Zfhx3*	0.2835558	3.554542	5.9682E-05	3.3775E-02
ENSMUSG00000026921	*Egfl7*	0.3844283	5.347486	8.1096E-05	4.1228E-02
ENSMUSG00000049907	*Rasl11b*	0.7504935	2.784222	9.0319E-05	4.3601E-02
ENSMUSG00000019997	*Ccn2*	0.6775769	5.56265	1.0405E-04	4.8659E-02
ENSMUSG00000000275	*Trim25*	0.281921	7.799913	1.1827E-04	4.9723E-02
ENSMUSG00000038473	*Nos1ap*	0.4494044	1.782445	1.1961E-04	4.9723E-02
DEGs downregulated in SmSEA-treated group (FDR < 0.05, logFC < 0)					
ENSMUSG00000049313	*Sorl1*	-0.4116065	8.519718	3.4660E-06	6.0348E-03
ENSMUSG00000066687	*Zbtb16*	-0.824671	2.989623	1.9177E-05	1.9369E-02
ENSMUSG00000007872	*Id3*	-0.4037403	5.731119	1.9318E-05	1.9369E-02
ENSMUSG00000022686	*B3gnt5*	-0.4908504	6.818884	1.9766E-05	1.9369E-02
ENSMUSG00000022508	*Bcl6*	-0.4840125	6.238576	1.9769E-05	1.9369E-02
ENSMUSG00000056313	*Tcim*	-0.4441411	4.686765	3.2725E-05	2.5725E-02
ENSMUSG00000024401	*Tnf*	-0.5088708	3.775864	4.4562E-05	2.7786E-02
ENSMUSG00000000617	*Grm6*	-0.4450148	2.299705	6.0938E-05	3.3775E-02
ENSMUSG00000029385	*Ccng2*	-0.2056347	6.328813	7.6171E-05	4.0711E-02
ENSMUSG00000015316	*Slamf1*	-0.3503705	4.448769	8.2649E-05	4.1228E-02
ENSMUSG00000005774	*Rfx5*	-0.2232814	6.671796	1.0835E-04	4.9136E-02
ENSMUSG00000043415	*Otud1*	-0.309302	4.459921	1.1308E-04	4.9723E-02

Abbreviations: FC – fold change; CPM – counts per million; FDR – false discovery rate.

renchyma (Fig. 1C and D), indicating a significant increase in alveolar septal wall thickness. The pro-inflammatory activity of heat denatured proteins has been reported previously (Yoon et al. 2008, Jozefowski and Marcinkiewicz 2010), which may explain this observation.

Scanned H & E stained lung sections were also analysed using the Positive Pixel Count algorithm (Aperio ImageScope software, Leica Biosystems, Mt Waverley, Australia) to determine the ratios of purple (nuclear) to red (cytoplasmic) staining as described previously (Yan et al. 2022). This analysis provides a measure of overt leukocyte infiltration, with no significant differences observed (Fig. 1E).

To ascertain whether SmSEA treatment might mediate transcriptional changes, RNA-seq was performed using the Illumina NextSeq 2000 platform as previously described (Dumenil et al. 2023, Bishop et al. 2024) on spleen and lung tissues harvested 5 dpi, where RNA from spleen and lung tissues was analysed independently. The RNA concentration and quality were checked using the 4200 TapeStation and RNA ScreenTape Kit (Agilent Technologies, Santa Clara, USA), with all the samples showing RNA integrity numbers greater than 9.3.

For the spleen samples, the average number of mapped reads per sample was 67.09 million (range 57.51–72.69 million). For the lung samples, the average number of mapped reads per sample was 59.48 million (range 48.75–68.90 million). Processed reads were aligned to GRCm39 vM31 (mouse genome) and the BA.5 genome using STAR aligner, with gene expression calculated using RSEM version 1.2.30 (Li and Dewey 2011).

Differential expression analysis between groups was performed using the quasi-likelihood pipeline from edgeR (3.40.2) (Chen et al. 2016) in R version 4.2.0. Only protein coding genes were selected from the RSEM expected counts and genes with low expression were filtered out of the dataset using edgeR's filterByExpr function. Filtered gene counts were input to edgeR and the design matrix model.matrix (~0 + Group) was used, where Group represented SmSEA, hiSmSEA or PBS, to compare gene expression between groups. No significant differences in the percentage of viral reads were observed in lung tissue between the groups (Fig. 1F).

Thirty-six differentially expressed genes (DEGs, FDR < 0.05) were identified in the spleens of the virus + SmSEA vs.

virus + PBS groups (Table 1). The upregulated genes in the SmSEA-treated mice included those encoding receptors for chemokines and interleukins (e.g., CXCR4 and Il10ra), anti-inflammatory modulators (e.g., Tsc22d3 and Zfp36l2), and pro-angiogenic molecules (e.g., Fosl2 and Egfl7), whereas the downregulated genes included Zbtb16, a gene that can promote inflammasome activity (Dong et al. 2023), and Tnf, a pro-inflammatory cytokine that has pleiotropic effects on various cell types.

The 36 DEGs were further analysed using Ingenuity Pathway Analysis (IPA, v84978992, QIAGEN). A number of annotations consistent with SEA immunomodulation (Janssen et al. 2016, Costain et al. 2018, Mu et al. 2021) was identified, including IL-10 Signalling, Macrophage Alternative Activation Signalling, Activin Inhibin Signalling Pathway, as well up-regulation (positive z-scores) of some Th2 (IL-4) and immunoregulatory (IL-10) cytokine response signatures, and downregulation (negative z-scores) of some Th1 cytokine signatures (IFNG, IL-18, and TNF) (Fig. 1G and Supplementary Table S1).

However, it should be noted that DEG numbers and fold changes were low, and z-scores only reached 2 for two of the annotations (IL-10 Signalling and Macrophage Alternative Activation Signalling), with upstream regulator annotations for some pro-inflammatory cytokines, IL-6, IL-1B and IL-2, also showing low positive z-scores (Fig. 1G and Supplementary Table S1).

Enrichment analysis of Gene Ontology (GO) Biological Process terms was performed using the enrichGO function from clusterProfiler version 4.6.2 (Wu et al. 2021). Terms such as the regulation of hematopoiesis, cytokine production, cell signalling and immune system process, and epithelial tube morphogenesis were significantly enriched (Supplementary Fig. S2, FDR < 0.05). These observations are thus consistent with what might be expected for SmSEA treatment but illustrate a marginal level of activity in this setting.

Twenty-one DEGs (FDR < 0.05) were identified in the spleens of the virus + SmSEA vs. virus + hiSmSEA groups (Supplementary Table S2). Among these DEGs, 10 (approximately 50%) were also present in the above-described DEG list (Table 1). Although the IPA results were compromised by low DEG numbers, the IL-10 signalling, Th1 and Th2 Activation Pathway, and IL-4 signature were retained. However, the TNF and IFNG signatures had low positive z-scores (suggesting upregulated activity) (Supplementary Table S3). This finding suggests that heat inactivation did not effectively eliminate SmSEA immunomodulatory activity in this setting, with a number of heat-insensitive SEA compounds previously identified (Kanse et al. 2005).

Differential expression analysis of lung RNA-seq data did not reveal any DEGs among the different groups, indicating that, when the current immunisation schedule and regime are used, SmSEA cannot improve pulmonary inflammatory responses in K18-hACE2 mice after SARS-CoV-2 infection. Additionally, classic angiogenic mediators, such as angiopoietins and vascular endothelial growth factor (VEGF), are elevated in COVID-19 patients and predictors of adverse outcomes (Madureira and Soares 2023). The pro-angiogenic nature of SmSEA (Loeffler et al. 2002, Kanse et al. 2005) may also limit its utility as a candidate for alleviating the pathology of COVID-19.

The study has some limitations such as the mice used were in a large range in ages and the experiment was performed only once. The findings of the study suggest that a single SmSEA inoculation, administered promptly after SARS-CoV-2 infection, can marginally modulate the cytokine response in the spleen of SARS-CoV-2-infected K18-hACE2 mice, as revealed by RNA-seq. However, no meaningful effects on cytokine responses or histopathology in infected lungs emerged.

The limited effects may suggest that the SmSEA dose administered in the study was too low. Alternatively, SARS-CoV-2 cytokine responses may be too robust, and SmSEA bioactivity may be intrinsically too weak to mediate meaningful therapeutic activity. The future work for use of HDPs as immunotherapeutics (Alghanmi et al. 2024) will require purification and manufacture of active ingredients (Ryan et al. 2022) and a series of scheduling and dosing evaluations (Buitrago et al. 2021).

Author´s contribution. Y. M.: writing – original draft, validation, methodology, investigation, formal analysis, data curation. K.Y.: validation, methodology, investigation, formal analysis, data curation. D.P.M.: funding acquisition, resources, conceptualisation. W.N.: methodology, formal analysis, data curation. D.J.R.: writing – review and editing, validation, methodology, data curation. J.A.R.: writing – review and editing, funding acquisition, conceptualisation. M.K.J.: writing – review and editing, validation, resources. P.C.: writing – review and editing, writing – original draft, visualisation, validation, supervision, funding acquisition, project administration, resources, methodology, investigation, formal analysis, data curation, conceptualisation.

Acknowledgements. We thank Mary Duke from the QIMR Berghofer Medical Research Institute for maintaining the *S. mansoni* life cycle. We thank the National Institute of Allergy and Infectious Diseases (NIAID) Schistosomiasis Resource Center of the Biomedical Research Institute (Rockville, MD) for providing *Oncomelania hupensis quadrasi* (Möllendorff) snails (NIH-NIAID Contract HHSN272201700014I) through BEI Resources. We thank Ross Koufariotis, Agnes Carolin, and the QIMR Berghofer Genome Informatics team, for their help in processing the RNA-sequencing data. We appreciate Sharon M. Hoyte and Rebecca L. Johnston at Medical Genomics, QIMRB, for their help in the bioinformatic analysis and critical review of the manuscript. We appreciate Andreas Suhrbier from QIMRB for thorough review of the manuscript. This work was supported by an Australian Infectious Disease Research Centre Seed Grant, a QIMR Berghofer Seed Grant and Grants (APP2008433 and APP1194462) from the National Health and Medical Research Council (NHMRC) of Australia. The funders had no role in the study design, data collection and analysis, decision to publish, or preparation of the manuscript.

REFERENCES

Adjobimey T., Meyer J., Terkes V., Parcina M., Hoerauf A. 2022: Helminth antigens differentially modulate the activation of CD4(+) and CD8(+) T lymphocytes of convalescent COVID-19 patients in vitro. BMC Med. 20: 241.

Alghanmi M., Minshawi F., Altorki T.A., Zawawi A., Alsaady I., Naser A.Y., Alwafi H., Alsulami S.M., Azhari A.A., Hashem A.M., Alhabbab R. 2024: Helminth-derived proteins as immune system regulators: a systematic review of their promise in alleviating colitis. BMC Immunol. 25: 21.

Bishop C.R., Dumenil T., Rawle D.J., Le T.T., Yan K., Tang B., Hartel G., Suhrbier A. 2022: Mouse models of COVID-19 recapitulate inflammatory pathways rather than gene expression. PLoS Pathog. 18: e1010867.

Bishop C.R., Yan K., Nguyen W., Rawle D.J., Tang B., Larcher T., Suhrbier A. 2024: Microplastics dysregulate innate immunity in the SARS-CoV-2 infected lung. Front. Immunol. 15: 1382655.

Buitrago G., Pickering D., Ruscher R., Cobos Caceres C., Jones L., Cooper M., Van Waardenberg A., Ryan S., Miles K., Field M., Dredge K., Daly N.L., Giacomin P.R., Loukas A. 2021: A netrin domain-containing protein secreted by the human hookworm *Necator americanus* protects against CD4 T cell transfer colitis. Transl. Res. 232: 88–102.

Cai P., Mu Y., McManus D.P. 2022: The fight against severe COVID-19: can parasitic worms contribute? Front. Immunol. 13: 849465.

Cao Z., Wang J., Liu X., Liu Y., Li F., Liu M., Chiu S., Jin X. 2024: Helminth alleviates COVID-19-related cytokine storm in an IL-9-dependent way. mBio 15: e00905–00924.

Chen Y., Lun A.T., Smyth G.K. 2016: From reads to genes to pathways: differential expression analysis of RNA-Seq experiments using Rsubread and the edgeR quasi-likelihood pipeline. F1000Res. 5: 1438.

Costain A.H., MacDonald A.S., Smits H.H. 2018: Schistosome egg migration: mechanisms, pathogenesis and host immune responses. Front. Immunol. 9: 3042.

Dharra R., Kumar Sharma A., Datta S. 2023: Emerging aspects of cytokine storm in COVID-19: the role of proinflammatory cytokines and therapeutic prospects. Cytokine 169: 156287.

Dong D., Du Y., Fei X., Yang H., Li X., Yang X., Ma J., Huang S., Ma Z., Zheng J., Chan D.W., Shi L., Li Y., Irving A.T., Yuan X., Liu X., Ni P., Hu Y., Meng G., Peng Y., Sadler A., Xu D. 2023: Inflammasome activity is controlled by ZBTB16-dependent SUMOylation of ASC. Nat. Commun. 14: 8465.

Duan T., Xing C., Chu J., Deng X., Du Y., Liu X., Hu Y., Qian C., Yin B., Wang H.Y., Wang R.-F. 2024: ACE2-dependent and -independent SARS-CoV-2 entries dictate viral replication and inflammatory response during infection. Nat. Cell. Biol. 26: 628–644.

Dumenil T., Le T.T., Rawle D.J., Yan K., Tang B., Nguyen W., Bishop C., Suhrbier A. 2023: Warmer ambient air temperatures reduce nasal turbinate and brain infection, but increase lung inflammation in the K18-hACE2 mouse model of COVID-19. Sci. Total Environ. 859: 160163.

Fogarty C.E., Zhao M., McManus D.P., Duke M.G., Cummins S.F., Wang T. 2019: Comparative study of excretory-secretory proteins released by *Schistosoma mansoni*-resistant, susceptible and naive *Biomphalaria glabrata*. Parasit. Vectors 12: 452.

Girgis N.M., Gundra U.M., Loke P. 2013: Immune regulation during helminth infections. PLoS Pathog. 9: e1003250.

Haeberlein S., Obieglo K., Ozir-Fazalalikhan A., Chayé M.A.M., Veninga H., van der Vlugt L.E.P.M., Voskamp A., Boon L., den Haan J.M.M., Westerhof L.B., Wilbers R.H.P., Schots A., Schramm G., Hokke C.H., Smits H.H. 2017: Schistosome egg antigens, including the glycoprotein IPSE/alpha-1, trigger the development of regulatory B cells. PLoS Pathog. 13: e1006539.

Hotez P.J., Brindley P.J., Bethony J.M., King C.H., Pearce E.J., Jacobson J. 2008: Helminth infections: the great neglected tropical diseases. J. Clin. Invest. 118: 1311–1321.

Janssen L., Silva Santos G.L., Muller H.S., Vieira A.R.A., De Camps T.A., De Paulo Martins V. 2016. Schistosome-derived molecules as modulating actors of the immune system and promising candidates to treat autoimmune and inflammatory diseases. J. Immunol. Res. 2016: 5267485.

Jozefowski S., Marcinkiewicz J. 2010: Aggregates of denatured proteins stimulate nitric oxide and superoxide production in macrophages. Inflamm. Res. 59: 277–289.

Kanse S.M., Liang O., Schubert U., Haas H., Preissner K.T., Doenhoff M.J., Dennis R.D. 2005: Characterisation and partial purification of *Schistosoma mansoni* egg-derived pro-angiogenic factor. Mol. Biochem. Parasitol. 144: 76–85.

Li B., Dewey C.N. 2011: RSEM: accurate transcript quantification from RNA-Seq data with or without a reference genome. BMC Bioinformatics 12: 323.

Loeffler D.A., Lundy S.K., Singh K.P., Gerard H.C., Hudson A.P., Boros D.L. 2002: Soluble egg antigens from *Schistosoma mansoni* induce angiogenesis-related processes by up-regulating vascular endothelial growth factor in human endothelial cells. J. Infect. Dis. 185: 1650–1656.

Madureira G., Soares R. 2023: The misunderstood link between SARS-CoV-2 and angiogenesis. A narrative review. Pulmonology 29: 323–331.

Mohammed E.S., Nakamura R., Kalenda Y.D.J., Deloer S., Moriyasu T., Tanaka M., Fujii Y., Kaneko S., Hirayama K., Ibrahim A.I., El-Seify M.A., Metwally A.M., Hamano S. 2020: Dynamics of serological responses to defined recombinant proteins during *Schistosoma mansoni* infection in mice before and after the treatment with praziquantel. PLoS Negl. Trop. Dis. 14: e0008518.

Mu Y., McManus D.P., Hou N., Cai P. 2021: Schistosome infection and schistosome-derived products as modulators for the prevention and alleviation of immunological disorders. Front. Immunol. 12: 619776.

Oyesola O.O., Hilligan K.L., Namasivayam S., Howard N., Clancy C.S., Zhao M., Oland S.D., Kiwanuka K.N., Garza N.L., Lafont B.A.P., Johnson R.F., Mayer-Barber K.D., Sher A., Loke P. 2023: Exposure to lung-migrating helminth protects against murine SARS-CoV-2 infection through macrophage-dependent T cell activation. Sci. Immunol. 8: eadf8161.

Qudus M.S., Tian M., Sirajuddin S., Liu S., Afaq U., Wali M., Liu J., Pan P., Luo Z., Zhang Q., Yang G., Wan P., Li Y., Wu J. 2023: The roles of critical pro-inflammatory cytokines in the drive of cytokine storm during SARS-CoV-2 infection. J. Med. Virol. 95: e28751.

Rawle D.J., Le T.T., Dumenil T., Yan K., Tang B., Nguyen W., Watterson D., Modhiran N., Hobson-Peters J., Bishop C., Suhrbier A. 2021: ACE2-lentiviral transduction enables mouse SARS-CoV-2 infection and mapping of receptor interactions. PLoS Pathog. 17: e1009723.

Ryan S.M., Ruscher R., Johnston W.A., Pickering D.A., Kennedy M.W., Smith B.O., Jones L., Buitrago G., Field M.A., Esterman A.J., McHugh C.P., Browne D.J., Cooper M.M., Ryan R.Y.M., Doolan D.L., Engwerda C.R., Miles K., Mitreva M., Croese J., Rahman T., Alexandrov K., Giacomin P.R., Loukas A. 2022: Novel antiinflammatory biologics shaped by parasite-host coevolution. Proc. Natl. Acad. Sci. U.S.A. 119: e2202795119.

Serrat J., Frances-Gomez C., Becerro-Recio D., Gonzalez-Miguel J., Geller R., Siles-Lucas M. 2023: Antigens from the helminth *Fasciola hepatica* exert antiviral effects against SARS-CoV-2 *in vitro*. Int. J. Mol. Sci. 24: 11597.

Siles-Lucas M., Gonzalez-Miguel J., Geller R., Sanjuan R., Perez-Arevalo J., Martinez-Moreno A. 2021: Potential influence of helminth molecules on COVID-19 pathology. Trends Parasitol. 37: 11–14.

Stewart R., Yan K., Ellis S.A., Bishop C.R., Dumenil T., Tang B., Nguyen W., Larcher T., Parry R., Sng J.J., Khromykh A.A., Sullivan R.K.P., Lor M., Meunier F.A., Rawle D.J., Suhrbier A. 2023: SARS-CoV-2 omicron BA.5 and XBB variants have increased neurotropic potential over BA.1 in K18-hACE2 mice and human brain organoids. Front. Microbiol. 14: 1320856.

Wolday D., Gebrecherkos T., Arefaine Z.G., Kiros Y.K., Gebreegzabher A., Tasew G., Abdulkader M., Abraha H.E., Desta A.A., Hailu A., Tollera G., Abdella S., Tesema M., Abate E., Endarge K.L., Hundie T.G., Miteku F.K., Urban B.C., Schallig H., Harris V.C., de Wit T.F.R. 2021: Effect of co-infection with intestinal parasites on COVID-19 severity: a prospective observational cohort study. EClinicalMedicine 39: 101054.

Wu T., Hu E., Xu S., Chen M., Guo P., Dai Z., Feng T., Zhou L., Tang W., Zhan L., Fu X., Liu S., Bo X., Yu G. 2021: clusterProfiler 4.0: a universal enrichment tool for interpreting omics data. Innovation (Camb) 2: 100141.

Yan K., Dumenil T., Tang B., Le T.T., Bishop C.R., Suhrbier A., Rawle D.J. 2022: Evolution of ACE2-independent SARS-CoV-2 infection and mouse adaption after passage in cells expressing human and mouse ACE2. Virus Evol. 8: veac063.

Yoon T.J., Kim J.Y., Kim H., Hong C., Lee H., Lee C.K., Lee K.H., Hong S., Park S.H. 2008: Anti-tumor immunostimulatory effect of heat-killed tumor cells. Exp. Mol. Med. 40: 130–144.

Received 3 February 2025 Accepted 10 April 2025 Published online 16 June 2025

Cite this article as: Mu Y., Yan K., McManus D.P., Nguyen W., Rawle D.J., Roberts J.A., Jones M.K., Cai P. 2025: Marginal cytokine modulation by *Schistosoma mansoni* soluble egg antigen in SARS-CoV-2-infected K18-hACE2 mice. Folia Parasitol. 72: 019.